

# Low energy states and the nature of the pseudogap in doped Mott insulators

Tiago C. Ribeiro

*Department of Physics, Massachusetts Institute of Technology, Cambridge, Massachusetts 02139, USA*

(Dated: May 23, 2019)

We show low energy states in doped Mott insulators can be understood in terms of spin-charge confined and spin-charge separated states. We then propose a simple two band picture to address the momentum space anisotropy and the unconventional nature of pseudogap states found in the cuprate materials. This picture amounts to interpreting the sharp disparity between the nodal and antinodal regions in terms of the distinction between spin-charge confined and spin-charge separated phenomenology. Our results are consistent with the chargeless character of excitations observed in hole and electron doped cuprates around  $(\pi, 0)$  and  $(\frac{\pi}{2}, \frac{\pi}{2})$  respectively.

The ubiquitous pseudogap in high- $T_c$  cuprates is manifested in a significant fraction of the unconventional phenomenology exhibited by these materials. However, understanding the physics underlying the presence of the pseudogap as well as the nature of pseudogap states is still an outstanding problem.

The suppression of low energy spectral weight corresponding to the pseudogap phenomenon is accompanied by the enhancement of the  $k$ -space anisotropy as observed by different experiments. [1, 2, 3, 4, 5, 6, 7] Moreover, in both hole and electron doped compounds the aforementioned anisotropy is reflected on the presence of unconventional states with depleted charge character in the pseudogap region of  $k$ -space. In fact, a variety of experimental probes consistently motivate that in superconducting hole doped materials quasiparticles in the nodal region couple to the superfluid density unlike the ones in the antinodal region. [8, 9, 10, 11] Interestingly, the roles of the zone diagonal and zone axis directions are interchanged when electron doped cuprates are considered instead. Indeed, the pseudogap is pushed toward the zone diagonal together with the chargeless excitations suggested by Raman spectroscopy and the violation of the Wiedemann-Franz law. [12, 13, 14] In the following we thus address the strong link between the  $k$ -space dependence of the pseudogap, the sharp  $k$ -space anisotropy present in normal and superconducting samples and the nature of states throughout the Brillouin zone (BZ) suggested by experiments in both hole and electron doped materials. [1, 2, 3, 4, 5, 6, 7, 8, 9, 10, 11, 12, 13, 14]

The pseudogap is increasingly more relevant as samples are underdoped and a popular school of thought advocates it stems from the proximity to the Mott insulating phase. The two-dimensional (2D) extended  $tJ$  model is often considered an appropriate starting point to tackle the physics of this strongly correlated problem. In particular, it proved useful in the study and comparison of both hole and electron doped regimes [15], including the different nature of excitations in the nodal region for either case [16] and the exotic character of antinodal states in hole doped materials. [17, 18, 19]

As such, below we consider the single hole 2D  $tt't''J$  model. For  $t' = t'' = 0$  this model yields a dispersion

along the magnetic Brillouin zone boundary (MBZB) which is too flat to match experiments. In addition, in this case the quasiparticle spectral weight at  $(\frac{\pi}{2}, \frac{\pi}{2})$  and  $(\pi, 0)$  are quite similar. [20, 21] However, upon introducing  $t' \sim -2t''$  a pseudogap opens and is followed by the decrease of quasiparticle spectral weight in the pseudogap region while the lower energy states away from the pseudogap maintain their quasiparticle-like properties. [17, 18, 19, 20] In this letter we propose a two band picture to understand these well known results. Specifically, we point out that the low energy states of such a doped Mott insulator are the superposition of states with sharp quasiparticle-like features and unconventional states with no quasiparticle-like behavior. We term the above Q and U (standing for “Quasiparticle” and “Unconventional” respectively) states. In the pseudogap region, increasing  $|t'|$  and  $|t''|$  is found to increase the energy of Q states but to have a limited effect on the energy of U states. As a result, the energy of the true eigenstates increases (further opening the pseudogap) as well as their overlap with U states (thus reducing quasiparticle spectral weight).

We also present evidence supporting that spin and charge are confined in Q states and separated in U states. The above described picture then allows us to assess the relevance of doping induced spin-charge separation in Mott insulators. In particular, our study found spin-charge separated states are relevant in the parameter regime concerning underdoped cuprates. Moreover, as we propose the rather distinct Q and U states predominate in different parts of  $k$ -space, our picture naturally leads to the sharp disparity between the nodal and antinodal regions. Furthermore, our results are valid for both hole and electron doped materials. For our purposes, the main distinction between the two regimes is that in the former the pseudogap opens in the antinodal region while in the latter it opens in the nodal region.

The single hole 2D  $tt't''J$  Hamiltonian is

$$H_{tJ} = - \sum_{\langle ij \rangle, \sigma} t_{ij} \left( \tilde{c}_{i,\sigma}^\dagger \tilde{c}_{j,\sigma} + H.c. \right) + \sum_{\langle ij \rangle} J_{ij} \mathbf{S}_i \cdot \mathbf{S}_j \quad (1)$$

where  $t_{ij}$  equals  $t$ ,  $t'$  and  $t''$  for first, second and third nearest neighbor sites respectively and vanishes otherwise.  $\tilde{c}_{i,\sigma}$  is the constrained operator  $\tilde{c}_{i,\sigma} = c_{i,\sigma}(1 -$

$n_{i,-\sigma}$ ). The exchange interaction only involves nearest neighbor spins for which  $J_{ij} = J$ . Units are set so that  $t = 1$ . To study this model we resort to both numerical and analytical techniques. Specifically, our results are supported by exact diagonalization (ED) of (1) on a  $4 \times 4$  lattice and by the self-consistent Born approximation (SCBA) approach on a  $16 \times 16$  lattice to the spinless-fermion Schwinger-boson representation of the  $tJ$  model. [21, 22] In the following  $|\psi_{\mathbf{k}}\rangle$  denotes the lowest energy state for each momentum in the ED calculation. Within the SCBA approach we truncate the quasiparticle wave function series after  $n = 3$  and use  $|\psi_{\mathbf{k}}\rangle \approx |\psi_{\mathbf{k}}^{(3)}\rangle / (\langle \psi_{\mathbf{k}}^{(3)} | \psi_{\mathbf{k}}^{(3)} \rangle)^{1/2}$ . [23] We leave all calculation details for a subsequent publication. [24]

A key observation is that increasing  $J$  enhances electron-like quasiparticle features of doped carriers. Hence, let  $G_{\mathbf{k}}$  denote the 2D Hilbert space generated by  $|\psi_{\mathbf{k}}, J, t', t''\rangle$  and  $\partial|\psi_{\mathbf{k}}, J, t', t''\rangle/\partial J$  for  $J > J_c(\mathbf{k}, t', t'')$ .  $J_c$  is the minimum value of  $J$  such that  $\langle \psi_{\mathbf{k}} | \tilde{c}_{\mathbf{k},\sigma} | \text{AF GS} \rangle \neq 0$ , where  $|\text{AF GS}\rangle$  is the undoped groundstate. Now consider the orthonormal states  $|Q_{\mathbf{k}}\rangle$  and  $|U_{\mathbf{k}}\rangle$  that form a basis of  $G_{\mathbf{k}}$ . They are uniquely determined by requiring  $\langle U_{\mathbf{k}} | \tilde{c}_{\mathbf{k},\sigma} | \text{AF GS} \rangle = 0$  (i.e. quasiparticle weight vanishes for  $|U_{\mathbf{k}}\rangle$ ). [25] For  $J < J_c$  the above construction does not apply and we simply set  $|\tilde{U}_{\mathbf{k}}\rangle \equiv |\psi_{\mathbf{k}}\rangle$ . In the following we show that spin and charge are confined in Q states ( $|Q_{\mathbf{k}}\rangle$ ) while they separate in U states ( $|U_{\mathbf{k}}\rangle$ ). We also find  $|\tilde{U}_{\mathbf{k}}\rangle$  describe spin-charge separated states.

Both ED and SCBA methods back up that  $G_{\mathbf{k}}$  does not change appreciably in a significantly large regime of the parameter  $J > J_c$ . [24] Thus, below we neglect the  $J$  dependence of  $|Q_{\mathbf{k}}\rangle$  and  $|U_{\mathbf{k}}\rangle$  (the dependence on  $t'$  and  $t''$  is kept). It is important to remark that the above construction is such that  $|Q_{\mathbf{k}}\rangle$  and  $|U_{\mathbf{k}}\rangle$  capture the physics for a fairly wide range of  $J$ .

To explore the physical properties of the above states first consider the spin density profile around the vacancy. As depicted in Fig. 1(a), in  $|Q_{\mathbf{k}}\rangle$  the vacancy freezes the surrounding antiferromagnetically ordered spins. On the other hand, in  $|U_{\mathbf{k}}\rangle$  the extra  $S^z = +\frac{1}{2}$  spin introduced by doping spreads away from the vacancy as it is illustrated in Fig. 1(b).

The above analysis is complemented by the study of the holon momentum distribution function. Figs. 1(c) and 1(d) depict  $n^h(\mathbf{q}) \equiv \langle U_{\mathbf{k}} | h_{\mathbf{q}}^\dagger h_{\mathbf{q}} | U_{\mathbf{k}} \rangle$ , where  $h_{\mathbf{q}}$  is the spinless holon destruction operator, with  $\mathbf{k} = (\frac{\pi}{2}, \frac{\pi}{2})$  and  $\mathbf{k} = (\pi, 0)$  respectively. Clearly, for U states such a distribution function is almost insensitive to total momentum. Additionally, holons are found to occupy states around  $(\pi, \pi)$  and, due to the long range AF order assumed within the SCBA, around  $(0, 0)$  as well. Actually, in Ref. 24 we extend the notion of holon momentum distribution to the ED formalism. In Table I we show the resulting holon momentum distribution function peaks

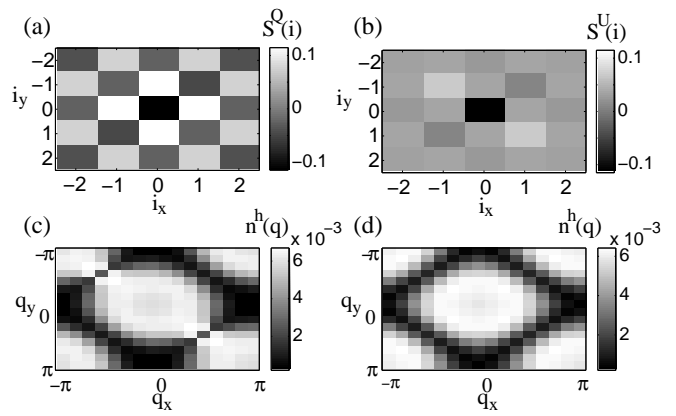


FIG. 1: (a)  $S^Q(\mathbf{i}) \equiv \langle Q_{\mathbf{k}} | \sum_j S_{j+i}^z \tilde{c}_{j,-1/2} \tilde{c}_{j,-1/2}^\dagger | Q_{\mathbf{k}} \rangle$  and (b)  $S^U(\mathbf{i}) \equiv \langle U_{\mathbf{k}} | \sum_j S_{j+i}^z \tilde{c}_{j,-1/2} \tilde{c}_{j,-1/2}^\dagger | U_{\mathbf{k}} \rangle$  where  $\mathbf{i}$  is the distance to the vacancy (black square at center),  $\mathbf{k} = (\frac{\pi}{2}, \frac{\pi}{2})$  and  $t', t'' = 0$ . Different  $\mathbf{k}$ ,  $t'$  and  $t''$  lead to qualitatively similar conclusions. [24] Holon momentum distribution ( $n^h(\mathbf{q})$ ) for  $|U_{\mathbf{k}}\rangle$  with (c)  $\mathbf{k} = (\frac{\pi}{2}, \frac{\pi}{2})$  and (d)  $\mathbf{k} = (\pi, 0)$ .

$\mathbf{k}$	$(\frac{\pi}{2}, \frac{\pi}{2})$	$(\pi, 0)$	$(\pi, \frac{\pi}{2})$	$(\frac{\pi}{2}, 0)$	$(0, 0)$
$\mathbf{q} = (0, 0)$	0.1192	0.1192	0.0676	0.1417	0.1280
$\mathbf{q} = (\pi, \pi)$	0.5442	0.5442	0.5860	0.5182	0.5714

TABLE I: Integrated holon momentum distribution function for  $|U_{\mathbf{k}}\rangle$ .  $\mathbf{q} = (0, 0)$  results involve sum over  $\mathbf{q} = (0, 0)$ ,  $\mathbf{q} = (\pm\frac{\pi}{2}, 0)$  and  $\mathbf{q} = (0, \pm\frac{\pi}{2})$ .  $\mathbf{q} = (\pi, \pi)$  results involve sum over  $\mathbf{q} = (\pi, \pi)$ ,  $\mathbf{q} = (\pm\frac{\pi}{2}, \pi)$  and  $\mathbf{q} = (\pi, \pm\frac{\pi}{2})$ . Based on ED calculation with  $t', t'' = 0$ . Equivalent results are obtained for  $t', t'' \neq 0$ . [24]

around  $\mathbf{q} = (\pi, \pi)$  for all  $\mathbf{k}$ . The results are dramatically different for Q states though. In fact, associated with the large quasiparticle weight, [26]  $\langle Q_{\mathbf{k}} | h_{\mathbf{q}}^\dagger h_{\mathbf{q}} | Q_{\mathbf{k}} \rangle$  is sharply peaked at  $\mathbf{q} = \mathbf{k}$ .

Hence, in  $|U_{\mathbf{k}}\rangle$  spin delocalizes as the spin background carries momentum while the charge lowers its kinetic energy by gathering around the bare band bottom. [27] This is remarkable evidence of a spin-charge separated state. Such a picture embeds small  $J$  physics and contrasts with the one described for Q states. In the latter momentum is carried by charge degrees of freedom while, away from the vacancy, AF correlations survive. The spin configuration around the vacancy additionally supports that spin and charge are tightly bound in these states which enclose large  $J$  physics. We further remark Q states emerge from strong correlation physics albeit their electron-like features for, in the paramagnetic state, they can be defined throughout the BZ and not just half of it as when the free electron picture applies.

The above real and momentum space features concerning U states were checked to hold even for the energy eigenfunctions  $|\psi_{\mathbf{k}}, J\rangle$  with  $J < J_c$ . [24] Hence,  $|\tilde{U}_{\mathbf{k}}\rangle$  also describe spin-charge separated states. As such, in some

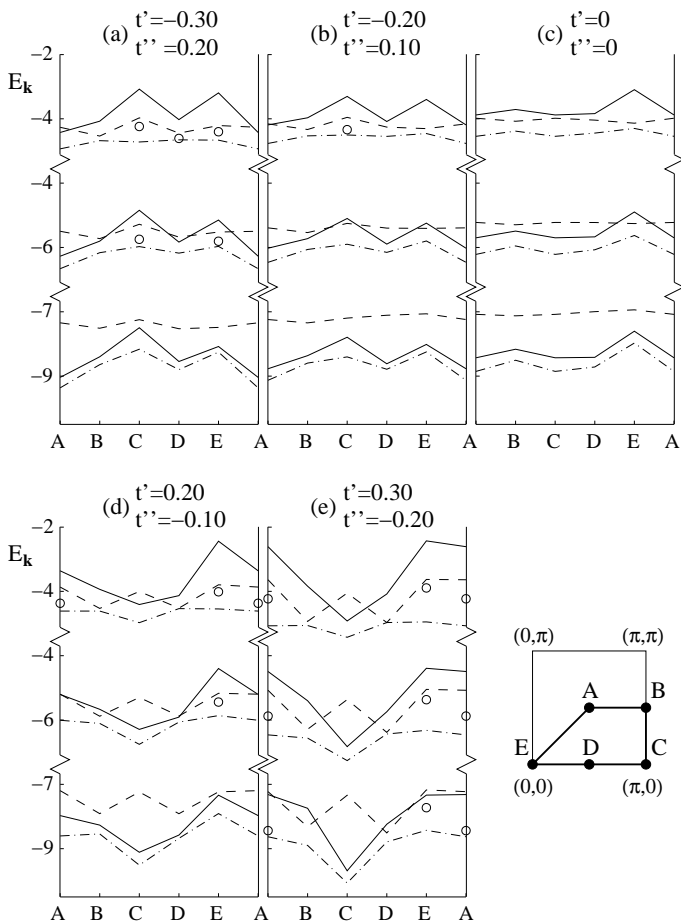


FIG. 2: Dispersion relations for  $|Q_{\mathbf{k}}\rangle$  (full line),  $|U_{\mathbf{k}}\rangle$  (dashed line) and  $|\psi_{\mathbf{k}}\rangle$  (dash-dot line). Upper, middle and lower set of dispersions are obtained for  $J$  equal to 0.2, 0.4 and 0.7 respectively. (a) is relevant to hole doped and (e) to electron doped cuprates. (o) indicates the best energy obtained by a linear combination of  $|Q_{\mathbf{k}}\rangle$  and  $|U_{\mathbf{k}}\rangle$  when  $J < J_c(\mathbf{k}, t', t'')$  (in which case  $|\psi_{\mathbf{k}}\rangle = |\tilde{U}_{\mathbf{k}}\rangle$ ).

$k$ -space regions true spin-charge separation is obtained for low enough  $J$ . [17, 18, 19] In addition, the previous conclusions regarding the nature of Q and U states are corroborated by the study of charge density and charge current correlation functions. [24]

In order to address the properties of the low energy sector of the doped Mott insulator in terms of Q and U states consider the dispersions  $E_{\mathbf{k}}^Q = \langle Q_{\mathbf{k}} | H_{t,J} | Q_{\mathbf{k}} \rangle$ ,  $E_{\mathbf{k}}^U = \langle U_{\mathbf{k}} | H_{t,J} | U_{\mathbf{k}} \rangle$  and  $E_{\mathbf{k}}^\psi = \langle \psi_{\mathbf{k}} | H_{t,J} | \psi_{\mathbf{k}} \rangle$  as given by ED (Fig. 2). [28] As expected, a larger  $J$  energetically favors  $|Q_{\mathbf{k}}\rangle$  with respect to  $|U_{\mathbf{k}}\rangle$ . Therefore,  $|\psi_{\mathbf{k}}\rangle$  becomes more Q-like as  $J$  is increased.  $E_{\mathbf{k}}^U$ , which is generally less dispersive than  $E_{\mathbf{k}}^Q$ , reflects the nature of the spin background as momentum is carried by the latter. Indeed, once doping induced frustration is more effective for  $t' < 0$  and  $t'' > 0$ ,  $E_{\mathbf{k}}^U$  is found to be softer in that regime. Moreover,  $E_{\mathbf{k}}^\psi$  closely follows  $E_{\mathbf{k}}^Q$  which derives from charge hopping processes in the presence of strong

$t'$	$t''$	$t'_{eff}$	$t''_{eff}$	$\Delta E^Q$	$\Delta E^\psi$	$W_{\mathbf{k}'}^Q$	$W_{\mathbf{k}''}^Q$
-0.3	0.2	-0.04	0.17	1.43	0.69	0	0.75
-0.2	0.1	-0.02	0.11	0.92	0.56	0.45	0.72
0	0	0.10	0.05	0	0	0.66	0.66
0.2	-0.1	0.24	0.00	-1.08	-0.75	0.76	0.50
0.3	-0.2	0.30	-0.12	-2.33	-0.80	0.82	0

TABLE II:  $t'_{eff}$  and  $t''_{eff}$  are determined from the best fit of the dispersion  $E_{\mathbf{k}} = E_0 + 4t'_{eff} \cos k_x \cos k_y + 2t''_{eff} (\cos 2k_x + \cos 2k_y)$  to  $E_{\mathbf{k}}^Q$  [29],  $\Delta E^Q \equiv E_{(\pi,0)}^Q - E_{(\pi/2,\pi/2)}^Q$ ,  $\Delta E^\psi \equiv E_{(\pi,0)}^\psi - E_{(\pi/2,\pi/2)}^\psi$  and  $W_{\mathbf{k}}^Q \equiv |\langle \psi_{\mathbf{k}} | Q_{\mathbf{k}} \rangle|^2$  with  $\mathbf{k} = \mathbf{k}' \equiv (\pi, 0)$  and  $\mathbf{k} = \mathbf{k}'' \equiv (\frac{\pi}{2}, \frac{\pi}{2})$  for several  $t'$  and  $t''$  and  $J = 0.4$ .

local AF correlations (as supported by the values of  $t'_{eff}$  and  $t''_{eff}$  in Table II).

Both Fig. 2 and Table II show the magnitude of the pseudogap ( $|E_{(\pi,0)}^\psi - E_{(\pi/2,\pi/2)}^\psi|$ ) as well as its location in  $k$ -space are controlled by  $t'$  and  $t''$ . [15, 30] Specifically, for  $t' < 0$  and  $t'' > 0$  the pseudogap is located around  $(\pi, 0)$  while for  $t' > 0$  and  $t'' < 0$  the pseudogap region is in the zone diagonal direction as observed in hole and electron doped materials respectively. [1, 14] In addition we find  $t'$  and  $t''$  induce similar changes on  $E_{\mathbf{k}}^Q$  and  $E_{\mathbf{k}}^\psi$  along the MBZB (compare, for instance,  $\Delta E^Q$  to  $\Delta E^\psi$  in Table II). The values of  $W_{\mathbf{k}}^Q$  for  $\mathbf{k} = (\pi, 0)$  and  $\mathbf{k} = (\frac{\pi}{2}, \frac{\pi}{2})$  in Table II also make it explicit that increasing the magnitude of the intrasublattice hopping parameters enhances the difference between states along the zone diagonal and zone axis directions. While pseudogap states have an increased spin-charge separated character, away from the pseudogap region the behavior gets more electron-like. The same understanding follows from the dependence of  $E_{\mathbf{k}}^Q - E_{\mathbf{k}}^U$  on  $t'$  and  $t''$  (Fig. 2) which control the pseudogap features.

The effect of  $t'$  and  $t''$  on the dispersions  $E_{\mathbf{k}}^Q$  and  $E_{\mathbf{k}}^U$  along the MBZB is easily understood in terms of the local properties of the spin background for each family of states. As illustrated in Fig. 1(a), in Q states the vacancy freezes the surrounding spins in a well defined staggered configuration so that the intrasublattice hopping parameters are only slightly renormalized (see the values of  $t'_{eff}$  and  $t''_{eff}$  in Table II). However, the fluctuation of spins around the vacancy in  $|U_{\mathbf{k}}\rangle$  (Fig. 1(b)) strongly renormalizes  $t'$  and  $t''$  in these states. Indeed, as depicted in Fig. 2,  $t'$  and  $t''$  change the dispersion  $E_{\mathbf{k}}^Q$  along the MBZB but not  $E_{\mathbf{k}}^U$ . In particular,  $t' < 0$  and  $t'' > 0$  lower  $E_{(\pi/2,\pi/2)}^Q$  and increase  $E_{(\pi,0)}^Q$ . The opposite holds for  $t' > 0$  and  $t'' < 0$ . The effect of increasing  $E_{\mathbf{k}}^Q$  is twofold. Firstly, it pushes  $E_{\mathbf{k}}^\psi$  upward. Secondly, it decreases the weight of  $|Q_{\mathbf{k}}\rangle$  in  $|\psi_{\mathbf{k}}\rangle$ . In addition, for large values of  $|t'|$  and  $|t''|$  the minimum energy obtained by a linear combination of  $|Q_{\mathbf{k}}\rangle$  and  $|U_{\mathbf{k}}\rangle$  in the pseudogap region is too high and a different state,  $|\tilde{U}_{\mathbf{k}}\rangle$ ,

becomes the groundstate (Fig. 2). Once  $|\tilde{U}_{\mathbf{k}}\rangle$  displays spin-charge separation the claim that increasing  $E_{\mathbf{k}}^Q$  enhances the spin-charge separation features of pseudogap states remains true. Naturally, decreasing  $E_{\mathbf{k}}^Q$  lowers  $E_{\mathbf{k}}^{\psi}$  and increases the weight of  $|Q_{\mathbf{k}}\rangle$  in  $|\psi_{\mathbf{k}}\rangle$ . Hence  $t'$  and  $t''$  render states close to the MBZB, but away from the pseudogap region, more Q-like. The intrasublattice hopping parameters thus have opposite effects around  $(\pi, 0)$  and  $(\frac{\pi}{2}, \frac{\pi}{2})$ .

To conclude, in this letter we show that within the extended  $tJ$  model the  $k$ -space anisotropy of states and the chargeless nature of pseudogap excitations are intrinsically linked to the presence of the pseudogap in accordance with experimental evidence. In particular, we address the sharp disparity between the nodal and antinodal regions in cuprates in terms of the distinction between spin-charge confined and spin-charge separated phenomenology. [18, 19] Our results support that  $t'$  and  $t''$  act in very different ways on Q and U states. These hopping parameters control the dispersion of the spin and charge bound state along the MBZB and, thus, the pseudogap magnitude, its spin-charge separated character and the  $k$ -space anisotropy as well. In addition,  $J$  is found to control the binding of the extra charge and spin introduced by doping. To understand the physics underlying the emergence of spin-charge separation features note that if the magnitude of  $t' \sim -2t''$  increase while  $J$  decreases the energy of the spin and charge bound state with pseudogap momentum gets higher and, at the same time, the binding between the spin and charge is weakened. As a result the system may prefer to minimize the charge kinetic energy which then separates from the extra spin.

The present calculation indicates that one of two scenarios holds in cuprates as we move along the MBZB toward the pseudogap region. Either  $|\langle\psi_{\mathbf{k}}|Q_{\mathbf{k}}\rangle|^2$  continuously decreases, without vanishing, considerably reducing the electron-like character of pseudogap states or, due to band crossing,  $|\langle\psi_{\mathbf{k}}|Q_{\mathbf{k}}\rangle|^2$  vanishes beyond a certain point thus leading to the presence of true spin-charge separation. We found  $|\langle\psi_{\mathbf{k}}|Q_{\mathbf{k}}\rangle|^2$  vanishes in the pseudogap region for  $t' = \pm 0.3, t'' = \mp 0.2, J = 0.4$  (these are experimentally relevant values). However, these results apply to the small  $4 \times 4$  lattice. Bigger systems are required to settle which of the above two scenarios is representative of real materials. Either way, spin-charge separation phenomenology is found to be important in underdoped cuprates.

Once  $E_{\mathbf{k}}^Q$  and  $E_{\mathbf{k}}^U$  cross each other around  $J \approx 0.4$  (Fig. 2) the underlying states strongly hybridize in the experimentally relevant parameter regime. To account for both

conventional quasiparticle-like and unconventional excitations we propose Q-like and U-like states should be used as building blocks of an effective theory for underdoped cuprates. The construction of such an effective model is the subject of a forthcoming publication. [31]

The author is grateful to Xiao-Gang Wen for several discussions and valuable comments on the manuscript. This work was partially supported by the Fundação Calouste Gulbenkian Grant No. 58119 (Portugal), NFSC Grant No. 10228408 (China), NSF Grant No. DMR-01-23156 and NSF-MRSEC Grant No. DMR-02-13282.

- 
- [1] A. Damascelli *et al.*, Rev. Mod. Phys. **75**, 473 (2003).
  - [2] L.B. Ioffe and A.J. Millis, Phys. Rev. B **58**, 11631 (1998).
  - [3] X.J. Zhou *et al.*, Phys. Rev. Lett. **92**, 187001 (2004).
  - [4] K. McElroy *et al.*, cond-mat/0406491.
  - [5] N. Gedik *et al.*, Science **30**, 1410 (2003).
  - [6] D. van der Marel, Phys. Rev. B **60**, 765 (1999).
  - [7] S. Ono and Y. Ando, Phys. Rev. B **67**, 104512 (2003).
  - [8] L.B. Ioffe and A.J. Millis, J. Phys. Chem. Solids **63**, 2259 (2002).
  - [9] L. Krusin-Elbaum *et al.*, Phys. Rev. Lett. **92**, 097005 (2004). L. Krusin-Elbaum *et al.*, cond-mat/0405416.
  - [10] Y. Gallais *et al.*, cond-mat/0403753.
  - [11] C. Panagopoulos *et al.*, Phys. Rev. B **67**, 220502 (2003).
  - [12] A. Koitzsch *et al.*, Phys. Rev. B **67**, 184522 (2003).
  - [13] R.W. Hill *et al.*, Nature **414**, 711 (2001).
  - [14] N.P. Armitage *et al.*, Phys. Rev. Lett. **88**, 257001 (2002).
  - [15] T. Tohyama, cond-mat/0406041.
  - [16] T.C. Ribeiro and X.-G. Wen, Phys. Rev. B **68**, 024501 (2003).
  - [17] G.B. Martins *et al.*, Phys. Rev. B **60**, R3716 (1999).
  - [18] T. Tohyama *et al.*, J. Phys. Soc. Jpn. **69**, 9 (2000).
  - [19] W.-C. Lee *et al.*, Phys. Rev. Lett. **91**, 057001 (2003).
  - [20] T. Tohyama and S. Maekawa, Supercond. Sci. Technol. **13**, R17 (2000).
  - [21] G. Martinez and P. Horsch, Phys. Rev. B **44**, 317 (1991).
  - [22] S. Schmitt-Rink *et al.*, Phys. Rev. Lett. **60**, 2793 (1988).
  - [23] A. Ramšak and P. Horsch, Phys. Rev. B **57**, 4308 (1998).
  - [24] T.C. Ribeiro, unpublished.
  - [25] This construction can be generalized to higher doping states and, eventually, to different lattice Hamiltonians as well.
  - [26] For all used model parameters we find  $0.5 \lesssim \frac{|\langle Q_{\mathbf{k}}|\tilde{c}_{\mathbf{k},\sigma}|\text{AF GS}\rangle|^2}{|\langle \text{AF GS}|\tilde{c}_{\mathbf{k},\sigma}^{\dagger}\tilde{c}_{\mathbf{k},\sigma}|\text{AF GS}\rangle|} \lesssim 0.8$  close to the MBZB.
  - [27] R. Eder *et al.*, Phys. Rev. Lett. **74**, 5124 (1995).
  - [28] We find it instructive to use  $|Q_{\mathbf{k}}\rangle$  and  $|U_{\mathbf{k}}\rangle$ , which are obtained for  $J > J_c$ , when  $J < J_c$  as well.
  - [29] Adding a  $t_{eff}$  term has only a small effect on  $t'_{eff}, t''_{eff}$ .
  - [30] K. Tanaka *et al.*, cond-mat/0312575.
  - [31] T.C. Ribeiro and X.-G. Wen, in preparation.